Tetrahedron Letters 49 (2008) 6448–6453

Contents lists available at ScienceDirect

Tetrahedron Letters

journal homepage: www.elsevier.com/locate/tetlet

A change in nucleotide selectivity pattern of porphyrin derivatives after immobilization on gold nanoparticles

Pavel Rezanka, Kamil Záruba, Vladimír Král *

Institute of Chemical Technology Prague, Department of Analytical Chemistry, Technická 5, 166 28 Prague 6, Czech Republic

ARTICLE INFO

Article history:
Received 2 July 2008
Revised 18 August 2008
Accepted 27 August 2008
Available online 31 August 2008

ABSTRACT

Two porphyrin-quaternized brucine salts **1** and **2** were immobilized on 3-mercaptopropanoic acid derivatized gold nanoparticles. The porphyrin modified nanoparticles were purified and characterized by a variety of techniques including electron microscopy and absorption spectroscopy in the UV–vis range. Interactions of nucleotides with **1** and **2** in solution and after immobilization of **1** and **2** on the surface of the nanoparticles were studied. A change in the selectivity pattern towards nucleotides as an effect of the porphyrin derivative immobilization is demonstrated.

1. Introduction

Studies of non-covalent intermolecular interactions in solution represent a modern approach to understanding fundamental forces and create a prerequisite for the development of supramolecular devices. It is well known that despite a long-term scientific effort, the selective binding of anions in general still represents a challenge because of their shape diversity and overall charge variability.[1,2] Chemical sensing of nucleotides, anionic building blocks of nucleic acids, is highly desirable in the fields of biology and medicine. Nucleotides play many essential roles in living cells, for instance, they participate in energy transfer processes, molecule activation, phosphate group transfer, etc.

Three characteristic features of nucleotides must be taken into consideration in nucleotide selector development; these are their ability to: (i) provide electrostatic interaction with a guest via a negatively charged phosphate group, (ii) participate in π–π aromatic interactions, and (iii) create hydrogen bonds based on adenine–thymine and guanine–cytosine complementarity. The majority of the selectors so far developed are based on urea, guanidinium or imidazolium units combined with rigid aromatic systems.[3–5] The aromatic moiety of the selectors binds to the aromatic part of the nucleotides and this induces spectral changes in their absorption and/or fluorescence spectra. Consequently, such derivatives have been successfully used for chemical sensing.[6] Oligopyrrolic macrocycles, specifically pendant nucleobase modified sapphyrins, are another family of selectors utilized successfully for nucleotide sensing.[7–9]

A quaternary ammonium group of a selector often constitutes its cationic centre interacting with the phosphate group of a nucleotide by an electrostatic interaction.[3] Several N-alkylated alkaloids have been successfully applied for recognition of carboxylates and phosphates, and represent a special case of the previously mentioned interaction principle.[10]

We have devoted considerable effort to the design of porphyrin-based selectors of biologically important species.[11,12] We prepared porphyrin-quaternized brucine salts **1** and **2** with remarkable behaviour in solution.[13,14] Spectroscopic and chromatographic experiments have proven the selective interaction of **1** with ATP in solution.[15]

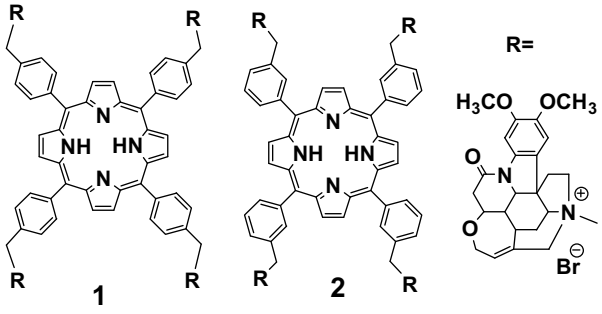

Metal nanoparticles play an important role in different areas of science, such as nanoelectronics, nonlinear optics, biological labelling and oxidation catalysis.[16] Nanoparticles themselves also provide a pragmatic approach to multiscale engineering, functioning as 'building blocks' of regular shape and size for the fabrication of larger structures.[17] Spherical gold nanoparticles (GNPs) with a size of 5–20 nm in diameter exhibit an intense red colour due to surface plasmon (SP) absorption, the result of collective oscillations of GNP surface electrons upon interaction with visible light of a suitable wavelength. The absorption coefficients of GNPs are

* Corresponding author. Tel.: +420 220 444 298; fax: +420 220 444 352.
E-mail address: Vladimir.Kral@vscht.cz (V. Král).

0040-4039/$ - see front matter © 2008 Elsevier Ltd. All rights reserved.
doi:10.1016/j.tetlet.2008.08.099

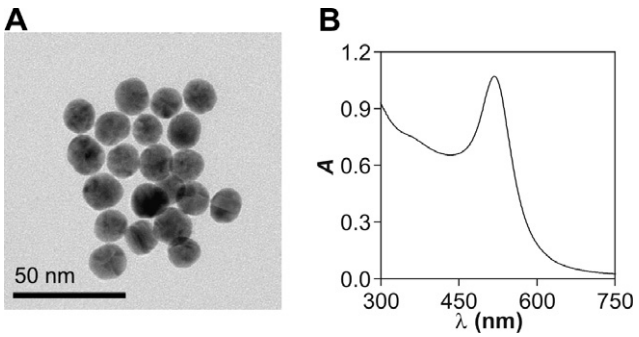

Figure 1. TEM image (A) and UV–vis spectrum in water (B) of GNPs prepared via method A.

nominally in the range of 10^8–10^{10} dm^3 mol^{-1} cm^{-1}.[18] Thus, they become an increasingly important colorimetric reporter to signify events associated with interactions of modified GNPs with analytes.[17] These recognition properties rely on the functional groups immobilized on the GNP surface.

Porphyrin-thiol derivatives can be used for the direct modification of gold surfaces[19–21] as well as GNPs.[22,23] In comparison to other types of nanoparticles, GNPs are very stable to oxidative degradation. On the other hand, they can be chemically modified almost exclusively by thio derivatives, which limits the number of available porphyrin derivatives. To overcome this drawback, reactive spacers are used for covalent as well as for non-covalent modification of the GNP surface.[21,24]

In the last decade many researchers have investigated the transferability of their knowledge gained on selective intermolecular recognition in solution to the area of solid support immobilized selectors/receptors potentially acting as chemical sensors.

2. Result and discussion

Herein, we present a supramolecular non-covalent approach for the modification of GNPs with porphyrin derivatives **1** and **2**. Modification of GNPs with 3-mercaptopropanoic acid is followed by non-covalent immobilization of **1** or **2**. The effect of GNPs on the interactions of **1** and **2** with nucleotides is described.

Gold nanoparticles prepared by a modified procedure originally published by Turkevitch et al.[25] (Section 3.1) were characterized by transmission electron microscopy (TEM) and UV–vis absorption spectroscopy (Fig. 1). The average diameter of the spherically shaped GNPs electrostatically stabilized with citrate was about 14.7 nm. The wavelength of the surface plasmon absorbance at 518 nm corresponds well with the average diameter estimated by TEM.[26]

GNPs covalently modified with salts of mercapto-substituted acids, for example, 3-mercaptopropanoic acid (MPA) and 10-mercaptodecanesulfonic acid, were used to enable subsequent non-covalent binding of polycationic species.[24,26] Here, citrate stabilized GNPs were modified with MPA in the molar ratio n(MPA)/n(Au) = 3. The modification was accompanied by a slight red shift of the plasmon absorption band of GNP-MPA (about 2 nm).[27]

Non-covalent binding of the porphyrin-brucine conjugates was carried out by adding a methanolic solution (2 mL) of **1** or **2** to GNP-MPA (100 mL) (Fig. 2).

Unbound species were removed by centrifugation followed by redispersion of the GNPs in a pure solvent, that is, water or methanol/HEPES solution (1:1 v/v). Compounds **1** and **2** have Soret

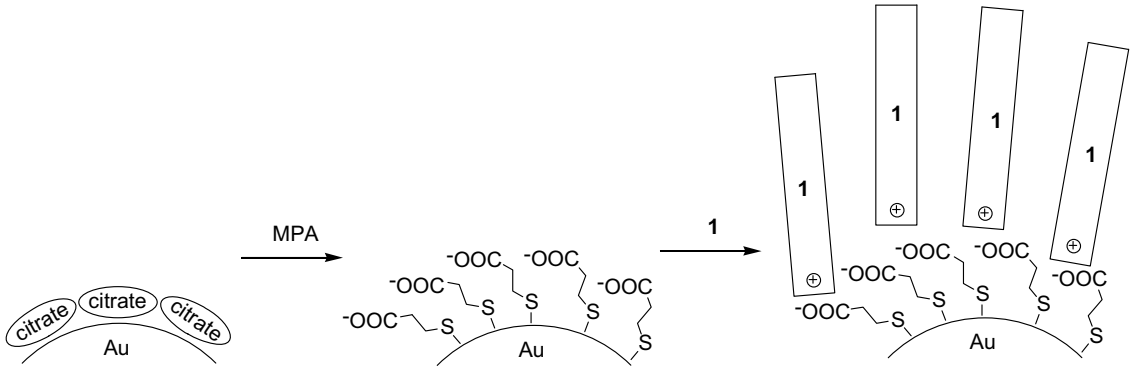

Figure 2. Representation of the two-step modification of GNPs.

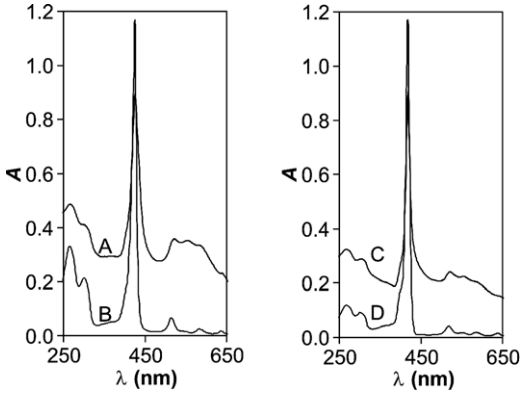

Figure 3. UV–vis spectra in aqueous solution; A—GNP-MPA-**1**; B—compound **1** (c = 3.9 μmol L^{-1}); C—GNP-MPA-**2**; D—compound **2** (c = 3.0 μmol L^{-1}).

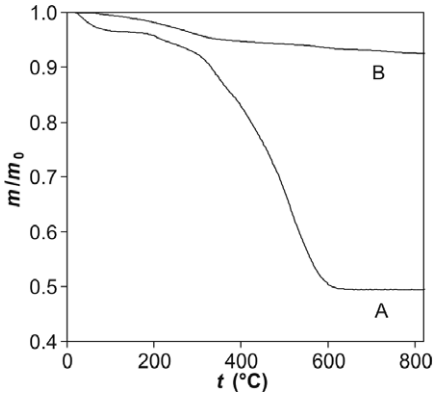

Figure 4. TGA of GNP-MPA-**1** (A); GNP-MPA (B).

bands at 425 and 418 nm, with bandwidths of 12 and 10 nm, respectively (Fig. 3). The Soret band of GNP-MPA-**1** in water was located at the same wavelength as **1** but broadened to 23 nm indicating some aggregation of porphyrins in the newly created layer.[23] The Q-bands of **1** and **2** were located at 514, 582, and 636 nm and the Q-bands of GNP-MPA-**1** and GNP-MPA-**2** were red-shifted to 521, 585, and 639 nm. Similarly, the shift of the surface plasmon absorbance to 555 nm after GNP modification can be ascribed to the increase of the GNP diameter.[27]

According to the thermogravimetric analysis (TGA) (Fig. 4), the number of immobilized molecules of compound **1** or **2** per one GNP was approximately 2800. This estimation was based on the observed loss of mass of GNP-MPA-**1** and GNP-MPA (Fig. 4), assuming that the Au(III) was completely reduced to form 14.7 nm-GNPs.

These results indicate a multilayer arrangement of **1** and **2** on GNPs. Such a hypothesis was confirmed by electronic circular dichroism (ECD) experiments. ECD spectra of aqueous solutions of **1** and **2** together with modified GNPs are shown in Figure 5. Due to the Soret absorption of **1** and **2** at 425 nm, negative and positive ECD signals can be observed in this region. GNP-MPA exhibits no ECD signal (spectrum C). In contrast to **1** and **2** in solution (spectra A and E), ECD signals of GNPs modified with **1** and **2** were significantly less intense (spectra B and D). This difference can be explained by the presence of chiral supramolecular assemblies of porphyrin-brucine conjugates in water as previously demonstrated for **1**.[13]

Surface-Enhanced Raman Spectroscopy (SERS)[28–30] was used for GNP surface characterization. The presence of GNPs in dilute aqueous solutions can enhance Raman signals by a factor of 10^4–10^6.[31] Moreover, the signal enhancement is strictly localized in the close vicinity of the surface. A vibrational study of the surface of the immobilized compounds is therefore possible.[28] Unfortunately, GNPs prepared by method A were too small to obtain SERS spectra with the 1024 nm excitation[32] used here to avoid undesirable fluorescence of **1** and **2**. Thus, larger GNPs were prepared by reduction of Au(III) at a lower concentration of citrate (Section 3.2). The resulting GNPs were polydisperse with an average diameter of about 45 nm and with the maximum of the surface plasmon absorbance at 552 nm (Fig. 6).

Figure 7 shows the Raman spectra of citrate, MPA and **1** and the SERS spectra of GNPs prepared by method B. The appearance of vibration bands at 653, 740, and 937 cm^{-1} and a shift of band structure around 1382 cm^{-1} in the spectrum of GNP-MPA

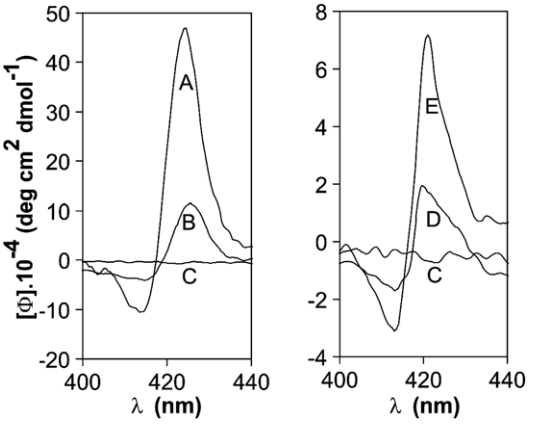

Figure 5. ECD spectra in aqueous solution. A—compound **1**; B—GNP-MPA-**1**; C—GNP-MPA; D—GNP-MPA-**2**; E—compound **2**.

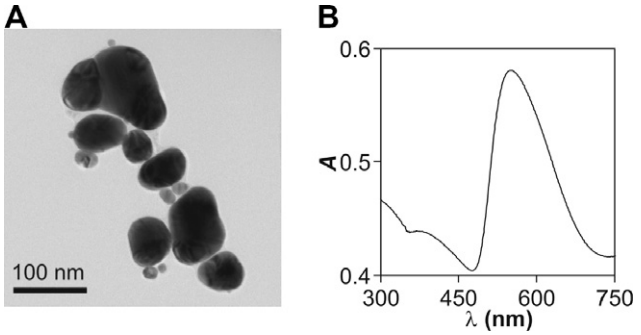

Figure 6. TEM image (A) and UV–vis spectrum in water (B) of GNPs prepared by method B.

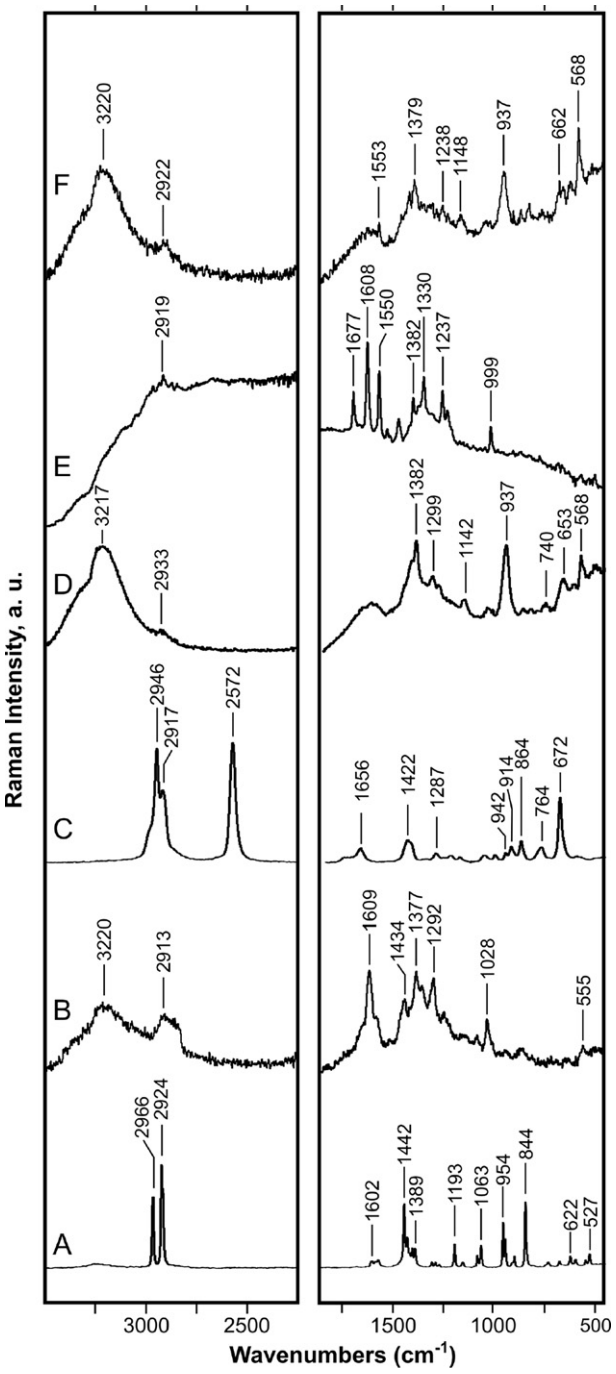

Figure 7. Raman spectra of citrate (A), GNPs/citrate (B), MPA (C), GNP-MPA (D), compound **1** (E) and GNP-MPA-**1** (F).

(spectrum D) compared with bands in the spectrum of citrate stabilized GNP (spectrum B) is related to the chemical modification of the nanoparticles with MPA (spectrum C).[33] Chemical reaction of MPA with the gold surface was also confirmed by the disappearance of the vibration band of the SH group at 2572 cm^{-1}. Since SERS spectra were measured in water, all the SERS spectra include the vibration band of water at about 3220 cm^{-1}. As can be seen by comparison of the Raman spectrum of pure **1** with the SERS spectra of GNP-MPA and GNP-MPA-**1** (Fig. 7), the spectra of GNP-MPA and GNP-MPA-**1** (spectrum F) are very similar. A few new bands (1238, 1553 cm^{-1}) in the spectrum of GNP-MPA-**1** can be tentatively assigned to non-covalently bonded **1**. An explanation of this similarity can be found in a strong localization of collective plasmon oscillations responsible for surface enhancement of Raman scattering to the surface.[28,29] There is a layer of MPA between the gold surface and the immobilized porphyrin derivatives. Consequently, SERS spectroscopy was not sensitive to porphyrin derivatives bonded relatively far from the surface (Fig. 2).

Interactions of GNP-MPA-**1** and GNP-MPA-**2**, both prepared by method A, with the nucleotides adenosine-5′-triphosphate (ATP) and adenosine-5′-diphosphate (ADP) and adenosine—(AMP), guanosine—(GMP), uridine—(UMP) and cytosine—(CMP) 5′-monophosphates were studied by UV–vis titrations in water and in methanol/HEPES solution (Section 3.5). The stock solutions of the modified GNPs were prepared in the appropriate solvent. The same solution was also used for the dissolution of the nucleotides so the concentration of the modified GNPs remained constant during the course of the titration. Individual absorption spectra were measured after the additions of the dissolved nucleotides into the stock solution of the modified GNPs (Fig. 8). The addition of the nucleotides caused a decline of the signal intensity at the absorbance maximum (Fig. 8).

Quantification of the interactions was based on the following model equation:

$$A = A_\infty - \frac{1}{K}\left(\frac{A - A_0}{C_N - \frac{C_P(A-A_0)}{A_\infty - A_0}}\right),$$

assuming 1:1 stoichiometry of the complex between the GNP-MPA-**1**, -**2** derivatives and the individual nucleotides,[15] where A is the actual absorbance, A_∞ is the theoretical absorbance when all of the GNP-MPA-modified porphyrin derivative is complexed with the nucleotide, K is the conditional constant, A_0 is the absorbance of the solution with no nucleotide present, c_N is the molar concentration of the nucleotide, and c_P is the molar concentration of the respective GNP-MPA-modified porphyrin derivative.

Values of conditional constants K and A_∞ in water were calculated using a nonlinear regression method[34] and are summarized in Table 1. In all cases the standard mean deviations of the estimated values were less than 10%. These data show significant differences in the interactions of immobilized **1** and **2** with the studied nucleotides. The estimated conditional constants K of all the nucleotides except for ADP are higher for GNP-MPA-**1** than for GNP-MPA-**2**. The highest K value indicates the strongest interaction between AMP and GNP-MPA-**1**. Unfortunately, the results with modified porphyrin derivatives immobilized on GNPs cannot be compared with measurements with free **1** and **2** because of their insufficient solubility in water.

Table 1
$K \cdot 10^{-3}$ and A_∞/A_0 (in parentheses) values of modified GNP complexes with nucleotides in water

	GNP-MPA-**1**	GNP-MPA-**2**
ATP	55 (0.59)	35 (0.45)
ADP	15 (0.57)	21 (0.74)
AMP	224 (0.65)	4 (0.73)
GMP	17 (0.62)	11 (0.81)
UMP	17 (0.77)	6 (0.84)
CMP	60 (0.67)	6 (0.83)

In our previous work,[15] we used a methanol/HEPES mixture to avoid problems with the very low solubility of **1** in water and to study interactions with adenosine nucleotides (AMP, ADP, and ATP). Here, we extended the group of nucleotides studied and experiments with free **2**, GNP-MPA-**1** and GNP-MPA-**2** were included. The results, obtained as described above, are summarized in Table 2.

Unlike the constants K in water, the estimated conditional constants for all the nucleotides are lower for GNP-MPA-**1** than for GNP-MPA-**2** in methanol/HEPES. K values for **2** were not evaluated due to the low change of absorbance except for the interaction with ATP. Several selected titration curves and the dependencies of A/A_0 on the chemical equivalents of ATP added, are presented

Table 2
$K \cdot 10^{-3}$ and A_∞/A_0 (in parentheses) values of various sample complexes with nucleotides in methanol/HEPES 1:1 (v/v) solution

	GNP-MPA-**1**	GNP-MPA-**2**	**1**	**2**
ATP	41 (0.58)	236 (0.75)	48 (0.42)	27 (0.93)
ADP	46 (0.81)	208 (0.79)	6 (0.63)	[a]
AMP	62 (0.88)	284 (0.84)	16 (0.92)	[a]
GMP	44 (0.85)	130 (0.89)	0.3 (0.84)	[a]
UMP	68 (0.89)	193 (0.85)	0.4 (0.58)	[a]
CMP	48 (0.92)	291 (0.91)	3 (0.85)	[a]

[a] Data not evaluated due to the low change of absorbance.

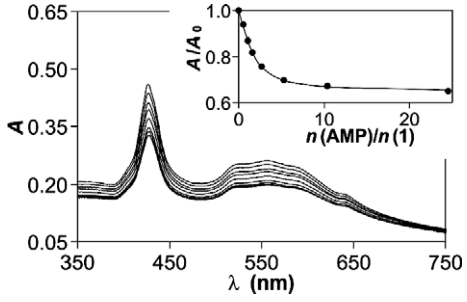

Figure 8. UV–vis spectra of GNP-MPA-**1** after additions of 0; 0.5; 1.0; 1.6; 2.7; 5.3; 10.4; 24.5 equiv of AMP. The inset shows the decrease of the A/A_0 ratio at 425 nm with the number of equivalents of AMP added. The concentration of GNP-MPA-**1** was kept constant (2 μmol L^{-1}).

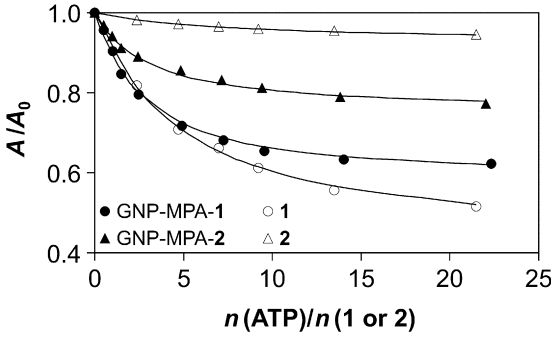

Figure 9. Changes in absorbance ratio (at the Soret band) upon the addition of ATP into methanol/HEPES 1:1 (v/v) solutions of **1**, **2**, GNP-MPA-**1**, and GNP-MPA-**2**. Plots denote measured data and a solid line is the calculated curve. A_0 is the absorbance of a solution without nucleotide.

in Figure 9. The interaction of **1** with ATP can be characterized by the conditional constant 48 000 and the A/A_0 ratio limits of 0.42, which are in good agreement with published results.[15] The immobilization of **1** onto nanoparticles (GNP-MPA-**1**) led to a slightly lower K value and the sensitivity (A/A_0 ratio at infinite nucleotide addition) for ATP also decreased. The sensitivity of the interaction of **2** with ATP was very low in methanol/HEPES (A_∞/A_0 ratio close to 1) but it increased after immobilization onto nanoparticles (Fig. 9). Unfortunately, the selectivity of the interaction of GNP-MPA-**1** with nucleotides studied in methanol/HEPES was lost and the selectivity of the interaction of immobilized **2** (GNP-MPA-**2**) was not observed. No K value was significantly higher than others (Table 2).

In conclusion, a supramolecular approach for the preparation of porphyrin-brucine modified gold nanoparticles by a two-step method is described. GNPs prepared by citrate reduction were modified with MPA. The porphyrin tetracation derivatives **1** and **2** were immobilized by Coulombic interactions with the carboxylate groups of MPA modified GNPs. A procedure for the isolation of the nanoparticles and spectroscopic characterization was developed. Interactions with nucleotides were studied by analysis of UV–vis absorption spectra. Immobilization of **1** and **2** on GNPs prevents the porphyrin derivatives from aggregation in water. Comparative experiments with free **1** and **2** versus GNP-MPA-**1**, GNP-MPA-**2** in methanol/HEPES revealed a strong influence of the immobilization of the porphyrin derivatives on their interactions with nucleotides. The strong selectivity of **1** for ATP in methanol/HEPES almost vanished if GNP-MPA-**1** was used instead. On the other hand, the interaction with AMP became stronger in both, GNP-MPA-**1** and GNP-MPA-**2** and it was further strengthened in the case of interaction with GNP-MPA-**1** in water The change of the binding selectivity of the porphyrin derivatives as a consequence of their immobilization on GNPs reflects the shift in the distribution of the peripheral positive charge on the porphyrin derivatives. While the free porphyrin derivatives use all the positively charged quaternary ammonium groups for anion binding, immobilization of the porphyrin derivatives through Coulombic interaction clearly uses some charged groups for attachment to the GNP surface leaving only a portion of the positively charged moieties available for anion binding. The observed change in selectivity from tri- to monophosphates as a result of immobilization can thus be rationalized.

3. Experimental

Methods A and B used were based on Au(III) reduction by citrate according to Turkevitch et al.[25]

3.1. Method A

To 100 mL of boiling water, 1 mL of a 1% aqueous solution of potassium tetrachloroaurate(III) and 2.5 mL of a 1% aqueous solution of trisodium citrate dihydrate were added. Heating was continued for 10 min during which time the solution changed colour from pale yellow to gray-blue, to purple and then to wine-red. The reaction vessel was allowed to cool to room temperature.

3.2. Method B

One percent aqueous solution (0.30 mL) of potassium tetrachloroaurate(III) and 0.11 mL of a 1% aqueous solution of trisodium citrate dihydrate were added to 30 mL of boiling water. Heating was continued for 30 min during which time the solution changed colour from pale yellow to gray-blue and then to brown. The reaction flask was allowed to cool to room temperature.

3.3. Nanoparticle derivatization with MPA

A solution of 3-mercaptopropanoic acid (MPA) (6.3 μL) in methanol (0.5 mL) and water (0.5 mL) was added to 100 mL of gold nanoparticles. The flask was capped and left to stand for 3 days in the dark at room temperature.

3.4. Immobilization of compounds 1 or 2

A solution of compound **1** or **2** (50 mg) in 2 mL of methanol was added to 100 mL of thiol modified gold nanoparticles. The flask was capped and left to stand for 3 days in the dark. Unbound species and reaction byproducts were then removed from the supernatant by centrifugation. The nanoparticles were repeatedly redispersed in water or methanol/HEPES (c = 1 mmol L^{-1}, pH 8.0) buffer mixture (1:1 v/v).

3.5. Interaction with nucleotides

Interactions of **1** and **2** in solution and after immobilization of **1** and **2** on nanoparticles were studied using UV–vis absorption spectroscopy. Experiments were carried out in water and in a methanol/HEPES (c = 1 mmol L^{-1}, pH 8.0) mixture (1:1 v/v). Concentrations of **1** (c = 3.9 μmol L^{-1}) or **2** (c = 3.0 μmol L^{-1}) were kept constant during addition of the nucleotide as the nucleotide was dissolved in the solution of **1** or **2**. A 1:1 stoichiometry of the complex modified porphyrin-nucleotide was assumed according to the published results.[15] Stability constants were estimated by nonlinear regression.[34]

Acknowledgements

The financial support from the Ministry of Education of the Czech Republic MŠMT 6046137307 and LC 512 and Grant Agency of the Czech Republic No. 203/06/0872 and KAN200100801 is gratefully acknowledged. The authors thank Dr. V. Setnička for assistance with ECD measurements and Dr. M. Klementova for TEM measurements.

References and notes

1. Katayev, E. A.; Ustynyuk, Y. A.; Sessler, J. L. *Coord. Chem. Rev.* **2006**, *250*, 3004–3037.
2. Beer, P. D.; Gale, P. A. *Angew. Chem., Int. Ed.* **2001**, *40*, 486–516.
3. Hirsch, A. K. H.; Fischer, F. R.; Diedrich, F. *Angew. Chem., Int. Ed.* **2007**, *46*, 338–352.
4. Kim, S. K.; Kim, H. N.; Xiaoru, Z.; Lee, H. N.; Lee, H. N.; Soh, J. H.; Swamy, K. M. K.; Yoon, J. *Supramol. Chem.* **2008**, *19*, 221–227.
5. Kwon, J. Y.; Singh, N. J.; Kim, H. N.; Kim, S. K.; Kim, K. S.; Yoon, J. *J. Am. Chem. Soc.* **2004**, *126*, 8892–8893.
6. Li, C.; Numata, M.; Takeuchi, M.; Shinkai, S. *Angew. Chem., Int. Ed.* **2005**, *44*, 6371–6374.
7. Král, V.; Sessler, J. L.; Furuta, H. *J. Am. Chem. Soc.* **1992**, *114*, 8704–8705.
8. Král, V.; Shishkanova, T. V.; Sessler, J. L.; Brown, C. T. *Org. Biomol. Chem.* **2004**, *2*, 1169–1175.
9. Sessler, J. L.; Genge, J. W.; Král, V.; Iverson, B. L. *Supramol. Chem.* **1996**, *8*, 45–52.
10. Lara, K. O.; Godoy-Alcántar, C.; Rivera, I. L.; Eliseev, A. V.; Yatsimirsky, A. K. *J. Phys. Org. Chem.* **2001**, *14*, 453–462.
11. Král, V.; Králová, J.; Kaplánek, R.; Bříza, T.; Martásek, P. *Physiol. Res.* **2006**, *55*, S3–S26.
12. Rusin, O.; Král, V. *Tetrahedron Lett* **2001**, *42*, 4235–4238.
13. Král, V.; Pataridis, S.; Setnička, V.; Záruba, K.; Urbanová, M.; Volka, K. *Tetrahedron* **2005**, *61*, 5499–5506.
14. Setnička, V.; Urbanová, M.; Pataridis, S.; Král, V.; Volka, K. *Tetrahedron: Asymmetry* **2002**, *13*, 2661–2666.
15. Kejík, Z.; Záruba, K.; Michalík, D.; Šebek, J.; Dian, J.; Pataridis, S.; Volka, K.; Král, V. *Chem. Commun.* **2006**, 1533–1535.
16. Daniel, M.-C.; Astruc, D. *Chem. Rev.* **2004**, *104*, 293–346.
17. Drechsler, U.; Erdogan, B.; Rotello, V. M. *Chem. Eur. J.* **2004**, *10*, 5570–5579.
18. Link, S.; El-Sayed, M. A. *J. Phys. Chem. B* **1999**, *103*, 4212–4217.
19. Ishida, A.; Majima, T. *Nanotechnology* **1999**, *10*, 308–314.
20. Viana, A. S.; Leupold, S.; Montforts, F. P.; Abrantes, L. M. *Electrochim. Acta* **2005**, *50*, 2807–2813.

21. Záruba, K.; Matějka, P.; Volf, R.; Volka, K.; Král, V.; Sessler, J. L. *Langmuir* **2002**, *18*, 6896–6906.
22. Akiyama, T.; Nakada, M.; Terasaki, N.; Yamada, S. *Chem. Commun.* **2008**, 395–397.
23. Kanehara, M.; Teranishi, T. e-J. *Surf. Sci. Nanotech.* **2005**, *3*, 30–32.
24. Kim, D. H.; Hernandez-Lopez, J. L.; Liu, J.; Mihov, G.; Zhi, L.; Bauer, R. E.; Grebel-Koehler, D.; Klapper, M.; Weil, T.; Muellen, K.; Mittler, S.; Knoll, W. *Macromol. Chem. Phys.* **2005**, *206*, 52–58.
25. Turkevitch, J.; Stevenson, P. C.; Hillier, J. *Discuss. Faraday Soc.* **1951**, *11*, 55–75.
26. Gittins, D. I.; Caruso, F. *J. Phys. Chem. B* **2001**, *105*, 6846–6852.
27. Templeton, A. C.; Pietron, J. J.; Murray, R. W.; Mulvaney, P. *J. Phys. Chem. B* **2000**, *104*, 564–570.
28. Moskovits, M. *Rev. Mod. Phys.* **1985**, *57*, 783–826.
29. Porter, M. D.; Lipert, R. J.; Siperko, L. M.; Wang, G.; Naraynan, R. *Chem. Soc. Rev.* **2008**, *37*, 1001–1011.
30. Ren, B.; Liu, G.-K.; Lian, X.-B. *Anal. Bioanal. Chem.* **2007**, 29–45.
31. Kneipp, K.; Kneipp, H.; Itzkan, I.; Dasari, R. R.; Feld, M. S. *Chem. Rev.* **1999**, *99*, 2957–2975.
32. Wei, A. e-J. *Surf. Sci. Nanotech.* **2006**, 9–18.
33. Kudelski, A. *J. Raman Spectrosc.* **2003**, *34*, 853–862.
34. Hirose, K. *J. Inclusion Phenom. Macrocycl. Chem.* **2001**, *39*, 193–209.